

Depth Profilometry of Near-Surface Inhomogeneities Via Laser-Photothermal Probing of the Thermal Diffusivity of Condensed Phases¹

A. Mandelis^{2,3} and M. Munidasa²

Several applications are presented of the Hamilton-Jacobi formulation of thermal-wave physics to the problem of laser photothermal depth profilometry of the thermophysical transport parameter (the thermal diffusivity) of inhomogeneous condensed phases (solids and liquids) with arbitrary, continuously varying thermal diffusivity profiles. A working general method for solving the inverse problem and obtaining arbitrary diffusivity depth profiles from the laser beam-intensity modulation frequency dependence of the photothermal signal (amplitude and phase) is described. Specific examples of profile reconstructions are presented, including magnetic field-induced thermophysical inhomogeneities in liquid crystals, laser processing inhomogeneities in steels and Zr-Nb alloys, and finally, evaluation of machining damage in metals. Whenever possible, profiles obtained photothermally are compared with those resulting from destructive methods, such as microhardness testing.

KEY WORDS: depth profiling; laser processing; liquid crystals; nondestructive evaluation; photothermal methods; shot-peening; thermal diffusivity.

1. INTRODUCTION

Photothermal and photoacoustic detection methods have evolved as a family of very effective nondestructive testing techniques complimentary to conventional methods such as ultrasound and x-ray inspection. These methods have advantages especially for near-surface detection with a variable depth range, compared to conventional techniques. In this family

¹ Invited paper presented at the Twelfth Symposium on Thermophysical Properties, June 19-24, 1994, Boulder, Colorado, U.S.A.

² Photothermal and Optoelectronic Diagnostics Laboratory, Department of Mechanical Engineering, University of Toronto, 5 King's College Road, Toronto, Ontario M5S 1A4, Canada.

³ To whom correspondence should be addressed.

of methods a beam of energy (laser or electron beam) modulated at a certain frequency is focused onto the sample surface. The resulting periodic heat flow in the material is a diffusive process, producing a periodic temperature distribution which is called a "thermal wave." Thermal waves are heavily damped, their amplitude decreasing by a factor of e^{-1} within a distance of one thermal diffusion length from the surface. The thermal diffusion length (penetration depth) μ is given by

$$\mu = \sqrt{\frac{\alpha}{\pi f}} \quad (1)$$

where α is the thermal diffusivity of the medium and f is the modulation frequency.

This frequency-dependent penetration depth has been utilized to reconstruct thermal diffusivity depth profiles from the frequency-domain surface temperature data. Even though much experimental work [1-4] and some theoretical models [2, 5] have been published regarding discontinuously inhomogeneous solids, theoretical implementation of realistic models addressing the equally important, and frequently more common, problem of continuously inhomogeneous solids has been less fertile. The most general and rigorous approach to the inverse thermal-wave problem has been given by Vidberg et al. [6]. This model uses the radial variation of the surface temperature of a continuously inhomogeneous solid about a heated point at a single modulation frequency. Both thermal conductivity and heat capacity profiles were reconstructed using Padé approximation for the inversion of spatial Laplace transforms. There are a number of constraints which limit the applicability of this model, the most significant constraints being that (i) it is valid only for nonconventional experimental geometry, (ii) the reconstructed profiles are not always numerically reliable, (iii) the accuracy is limited to a depth reconstruction on the order of one diffusion length, and (iv) the reconstruction algorithm is relatively complex and is sensitive to the presence of small amounts of error.

A reconstruction method based on the classical mechanical concept of the Hamilton-Jacobi thermal harmonic oscillator (THO) has been reported [7]. In this paper we report progress made in the application of the depth profiling method described in Ref. 7. The depth-profiling thermal-wave problem for continuously thermally varying solids in the conventional frequency-domain photothermal spectrometry is addressed, using either the photoacoustic gas-cell or the photothermal radiometric detection method. Unlike earlier treatments, well-posed, direct, simple, and convenient expressions for the frequency dependence of the photothermal signal have been obtained. Simple numerical (some cases analytical)

inversions of amplitude and phase data can yield thermal diffusivity spatial profiles by means of a self-adjusting method based on the experimental modulation frequency response of optically opaque continuously inhomogeneous samples. This allows profile reconstructions largely independent of assumed specific mathematical profiles.

2. THEORETICAL APPROACH: RECONSTRUCTION METHOD OF THERMAL DIFFUSIVITY PROFILES

The solution to the thermal diffusion equation in a semiinfinite solid medium with continuously variable thermal conductivity, $k(x)$, density $\rho(x)$, and specific heat, $c(x)$, which is excited by a photothermal source at an intensity modulation angular frequency ω , based on the THO model leads to an expression for surface temperature $T(0, \omega)$ given by [8]

$$T(0, \omega) = T_0(\omega) \left\{ 1 + \frac{1}{4} R^{1/2}(\infty) \exp \left[-\frac{(1+i)\sqrt{\omega}}{2\sqrt{2}q} \frac{1}{\sqrt{\alpha_x}} \ln \left(\frac{\alpha_0}{\alpha_x} \right) \right] \right\} \quad (2)$$

In deriving this equation a specific convenient monotonically decreasing thermal diffusivity profile, $\alpha_s(x) = k_s(x)/\rho_s(x) c_s(x)$, given by

$$\alpha_s(x) = \alpha_0 \left(\frac{1 + \Delta e^{-qx}}{1 + \Delta} \right)^2; \quad \Delta \equiv \left(\frac{\alpha_0}{\alpha_x} \right)^{1/2} - 1 \quad (3)$$

was assumed. Here α_0 and α_x are thermal diffusivities at the surface ($x=0$) and bulk, respectively, and q determines the rate of changes of $\alpha_s(x)$. In Eq. (2)

$$R(x) \equiv e_s(0)/e_s(x) \quad (4)$$

where $e_s(x)$ is the depth-dependent thermal effusivity, $e_s(x) = [k(x) \rho(x) c(x)]^{1/2}$, and $T_0(\omega)$ is interpreted as the surface temperature of the condensed medium with homogeneous $\alpha_s(x) = \alpha_0$. The surface temperature of a homogeneous medium of diffusivity α_j and conductivity k_j due to an incident energy flux of Q_0 is given by

$$T_0(\omega) = \frac{Q_0}{k_j \sigma_j}; \quad j = 0 \text{ or } \infty \quad (5)$$

where $\sigma_j = (1+i)(\omega/2\alpha_j)^{1/2}$. Then the frequency response signal of a continuously thermally inhomogeneous solid sample when normalized by the

response of a homogeneous reference sample (with thermal diffusivity α_x) is given upon division of Eq. (2) by Eq. (5) with $j = \infty$:

$$|M(\omega)| e^{i \Delta\phi(\omega)} = \frac{1}{R(\infty)} \left\{ 1 + \frac{1}{4} R^{1/2}(\infty) \exp \left[-\frac{(1+i)\sqrt{\omega}}{2\sqrt{2}q} \frac{1}{\sqrt{\alpha_x}} \ln \left(\frac{\alpha_0}{\alpha_x} \right) \right] \right\} \quad (6)$$

where $|M(\omega)|$ is the amplitude ratio and $\Delta\phi(\omega)$ is the phase difference.

Although this expression is valid for a monotonically decreasing thermal diffusivity depth profile given by Eq. (3), arbitrary $\alpha_x(x)$ profiles can be handled by redefining (updating) two of the three constants q , α_0 , and α_x at every modulation frequency f_j . Here we can consider two types of samples.

2.1. Surface Inhomogeneities

Most engineering materials, such as laser processed [9, 10] and shot-peened metals and alloys, fall into this category. In these materials inhomogeneity starts from the surface and approaches the homogeneous bulk diffusivity of the original material. In this case α_x is assumed to be known and so is the thermal diffusivity of the homogeneous reference sample and the bulk diffusivity of the sample under investigation. Here the constants to be calculated at each frequency are q and α_0 . Equation (6) has to be solved numerically.

2.2. Bulk Inhomogeneities

This is a special case where the sample surface is unchanged and remains as the original (reference) sample and the bulk is inhomogeneous. One example, results of which are discussed later, is related to the magnetic field-induced thermal inhomogeneities in liquid crystals [11]. Here the constants to be calculated at each frequency are q and α_x . Since the reference sample diffusivity is the same as the constant surface diffusivity, α_0 , of the inhomogeneous sample, upon division of Eq. (2) by Eq. (5), we obtain

$$|M(\omega)| e^{i \Delta\phi(\omega)} = 1 + \frac{1}{4} R^{1/2}(\infty) \exp \left[-\frac{(1+i)\sqrt{\omega}}{2\sqrt{2}q} \frac{1}{\sqrt{\alpha_x}} \ln \left(\frac{\alpha_0}{\alpha_x} \right) \right] \quad (7)$$

It is possible to solve this for q and α_x analytically using data from neighboring frequencies, such that [11]

$$\omega_{j-1} = \omega_j - \delta\omega; \quad \delta\omega \ll \omega_j \quad (8)$$

For both cases given in Sections 2.1 and 2.2, it is assumed that the effusivity ratio, $R(\infty)$, at $x = \infty$ and $x = 0$, is adequately represented by the respective conductivity ratio, resulting in the relation

$$R(\infty) = \sqrt{\frac{\alpha_0}{\alpha_x}} \tag{9}$$

The calculation of the depth x_j is based on the fact that as modulation frequency decreases, the thermal wave probing depth (thermal diffusion length) $\mu_j = \mu(\omega_j)$, Eq. (1) increases. Starting from the highest practical frequency ω_1 , i.e., the shortest $x_1 \sim \mu_1$, we can write

$$x_1 = \mu_1 \equiv [2(\alpha_0)_1/\omega_1]^{1/2} \tag{10}$$

where a surface slice is approximated with $\alpha_s(x) = (\alpha_0)_1$. With decreasing frequency $f_j < f_{j-1}$, an increase in depth is given by

$$\mu_j = \mu_{j-1} + \sqrt{\frac{2\alpha_j}{\omega_j}} - \sqrt{\frac{2\alpha_{j-1}}{\omega_{j-1}}} \tag{11}$$

3. EXPERIMENTAL METHOD

Most of the results presented here are based on the photothermal radiometric detection method [12]. A schematic diagram of the experimental apparatus is shown in Fig. 1 [10]. An Ar⁺ laser modulated by an

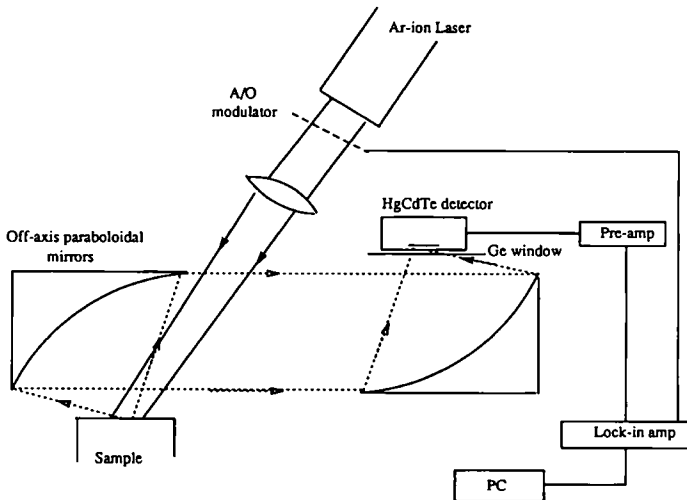


Fig. 1. Schematic diagram of the photothermal radiometric detection system.

acoustooptic (A/O) modulator is directed onto the sample surface. The radiation emitted by the sample surface is collected and focused onto the detector using two off-axis parabolic mirrors. The detector is a liquid N₂-cooled HgCdTe element with an active area of 1 mm² and a spectrally sensitive range of 2–24 μm. A germanium window with a transmission bandwidth of 2–13 μm is mounted in front of the detector to block any visible radiation from the pump laser. The pump beam spot size is made larger than the maximum profiling depth to maintain the one-dimensional heat diffusion formalism assumed in the theory. The detector signal is preamplified before being sent into a lock-in amplifier. The lock-in amplifier outputs, amplitude and phase are recorded at a range of laser modulation frequencies.

4. RESULTS

This depth profiling technique has been applied successfully to several samples of industrial and scientific interest such as laser processed Zr alloys [10], shot-peened steels, steels with surface modification due to machining, and magnetic field-induced depth profiles in liquid crystals [11].

Laser processing of materials is of interest in many industrial applications where a surface layer is modified to obtain improved properties, such

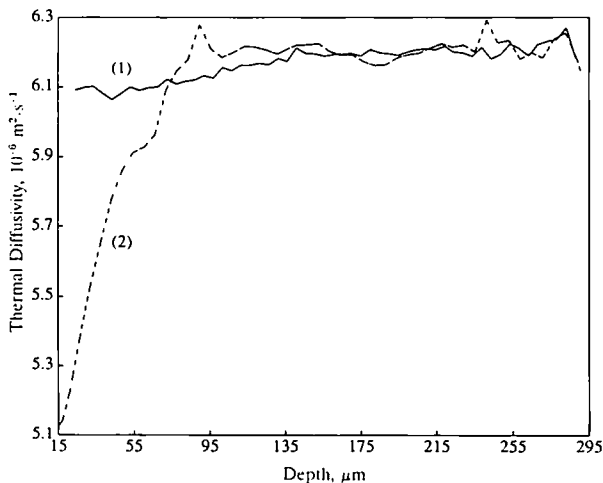


Fig. 2. Reconstructed thermal diffusivity profiles of two laser-processed Zr-2.5Nb alloy samples: (1) processed with a 1.5-kW CO₂ laser with no surface preparation; (2) surface blasted with 8-μm glass beads before processing. Processing parameters were the same as in sample 1.

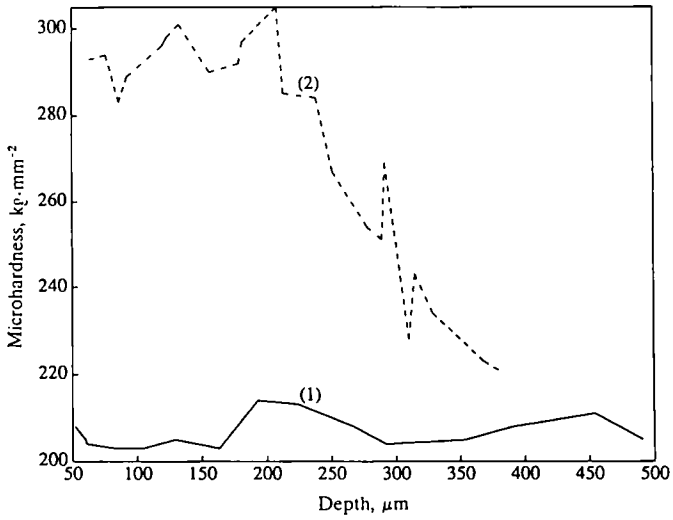


Fig. 3. Hardness obtained from the Vickers hardness test vs depth for cross sections of samples 1 and 2 in Fig. 2.

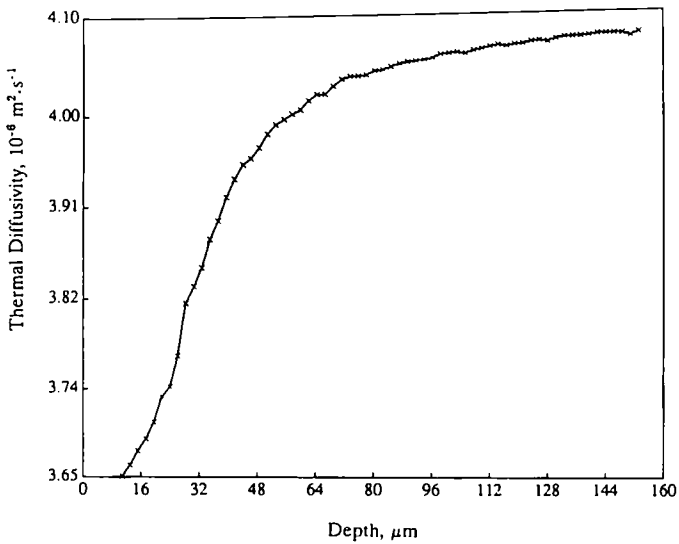


Fig. 4. Reconstructed thermal diffusivity profile of a shot-peened stainless-steel sample.

as hardness, corrosion resistance, and fatigue strength, while the base material remains in the original condition. Thermal conductivity, which depends on the transport properties of the material, is very sensitive to changes that take place in the material as a result of laser processing. Considering this change in the thermal conductivity, hence in the diffusivity, and the typical depths of hardened layers involved, photothermal radiometry [12] was considered an appropriate nondestructive method by which to profile these subsurface inhomogeneities. Figure 2 shows diffusivity profiles of two laser-processed Zr-2.5Nb alloy samples obtained using Eq. (6). Both samples were laser processed in vacuum using a 1.5-kW CO₂ laser, but sample No. 2 was blasted with 8- μ m glass beads before laser processing to enhance the laser absorption. After laser processing both sample surfaces looked similar visually. Thermal diffusivity profiles clearly show the effect due to enhanced laser absorption. Figure 3 shows the corresponding microhardness profiles of the same samples. It is difficult to make reliable hardness measurements very close to the edge (below 50 μ m) of the sample cross section, a definite advantage of photothermal depth profilometry.

Shot-peening is another surface hardening method where the material surface is bombarded with small solid pellets. Figure 4 shows a thermal diffusivity profile reconstructed from the photothermal radiometric data obtained from a shot-peened stainless steel sample using Eq. (6). Figure 5 is the corresponding microhardness profile showing a good anti-correlation with the diffusivity profile. A similar trend in thermal diffusivity decreasing with increase in hardness in carbon steel has been reported earlier [13].

Thermal diffusivity profile reconstructions from both sides of a stainless-steel plate machined to a thickness of 250 μ m are shown in Fig. 6; Eq. (6) was used here. The machining process appears to disturb the thermophysical properties of low-carbon steel down to a depth of ca. 30 μ m.

Figure 7 shows photoacoustic signal phase difference between a nematic liquid crystal octylcyanobiphenyl (8CB) sample at 37.5 °C with an applied transverse magnetic field $B = 1.65$ kG and the same sample with $B = 0$, as a function of laser modulation frequency [11]. These data have been obtained by placing the sample in a photoacoustic gas cell [14]. Figure 8 shows the thermal diffusivity profile reconstructed from those data, using the imaginary part of Eq. (7). These observations were found to be in agreement with the trends in thermal conductivity observed in other liquid crystal measurements [15, 16]. This depth profiling technique was able to measure the extent of the magnetic field-induced effects, for the first time.

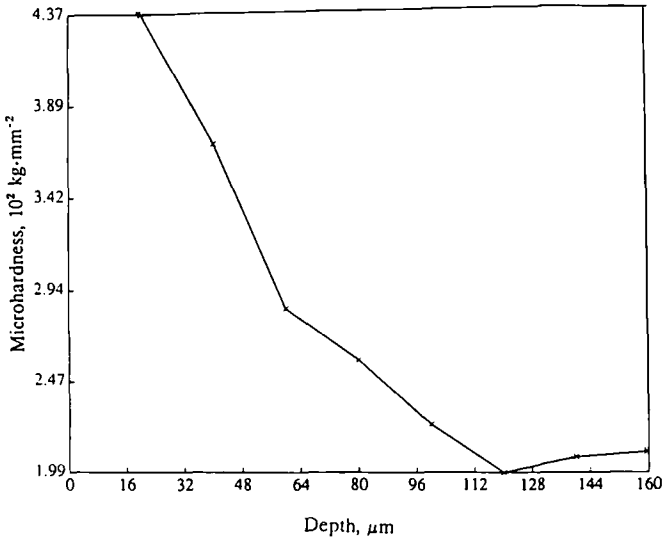


Fig. 5. Hardness obtained from the Vickers hardness test vs depth for cross sections of the sample in Fig. 4.

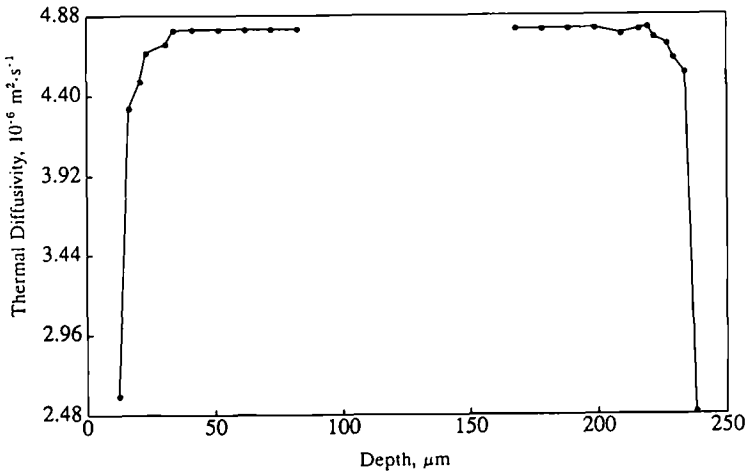


Fig. 6. Reconstructed thermal diffusivity profile from a machined steel plate of thickness $250 \mu\text{m}$ showing the effect of machining.

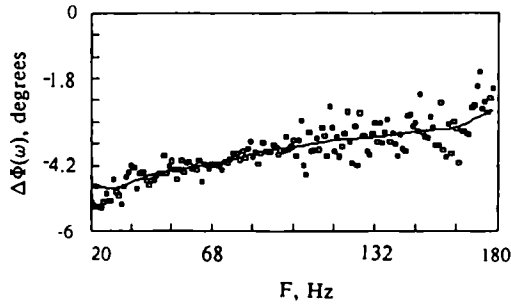


Fig. 7. Photoacoustic signal phase difference between a nematic 8CB sample at 37.5 °C with an applied transverse magnetic field $B = 1.65$ kG and the same sample with $B = 0$. The solid line is the smoothed data.

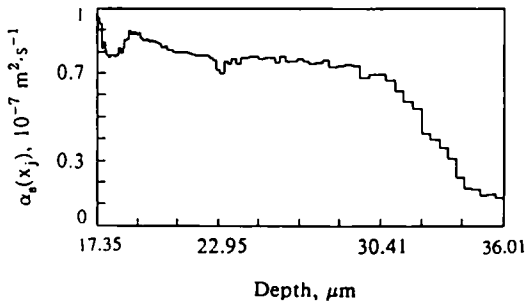


Fig. 8. Thermal diffusivity profile of a nematic 8CB sample with a transverse magnetic field of 1.65 kG at 37.5 °C reconstructed from the data in Fig. 7.

5. CONCLUSIONS

In this paper we have presented a reliable nondestructive remote sensing laser photothermal technique, embodied by infrared radiometry or photoacoustic detection, which allows the reconstruction of thermal diffusivity profiles in an inhomogeneous sample. Although a monotonically decreasing diffusivity profile [Eq. (3)] is assumed theoretically for analytical calculations, we have shown that our algorithm can handle arbitrary profiles, owing to the local adjustment of the values α_0 (or α_x) and q at every experimental frequency.

To improve the power of this technique as a quantitative tool for depth profiling, it is necessary to relate thermal diffusivity to actual physical

changes taking place within the material. Therefore, it is important to direct future work toward studying the effects on thermal diffusivity of changes in microstructure, grain size, residual stress, hardness, etc.

ACKNOWLEDGMENT

We wish to acknowledge gratefully the support of the Manufacturing Research Corporation of Ontario.

REFERENCES

1. S. D. Campbell, S. S. Yee, and M. A. Afromowitz, *IEE Trans. Biomed. Eng.* **BME-26**:220 (1979).
2. J. Opsal and A. Rosencwaig, *J. Appl. Phys.* **53**:4240 (1982).
3. A. Mandelis and J. D. Lymer, *Appl. Spectrosc.* **39**:473 (1985).
4. J. Baumann and R. Tilgner, *Can. J. Phys.* **64**:1291 (1986).
5. A. Mandelis, Y. C. Teng, and B. S. H. Royce, *J. Appl. Phys.* **50**:7138 (1979).
6. H. J. Vidberg, J. Jaarinen, and D. O. Riska, *Can. J. Phys.* **64**:1178 (1986).
7. A. Mandelis, *J. Math. Phys.* **26**:2676 (1985).
8. A. Mandelis, S. B. Peralta, and J. Thoen, *J. Appl. Phys.* **70**:1761 (1991).
9. T. C. Ma, M. Munidasa, and A. Mandelis, *J. Appl. Phys.* **71**:6029 (1992).
10. M. Munidasa, T. C. Ma, A. Mandelis, S. K. Brown, and L. Mannik, *Mater. Sci. Eng.* **A159**:111 (1992).
11. A. Mandelis, E. Schoubs, S. B. Peralta, and J. Thoen, *J. Appl. Phys.* **70**:1771 (1991).
12. W. P. Leung and A. C. Tam, *J. Appl. Phys.* **56**:153 (1984).
13. J. Jaarinen and M. Lukkala, *J. Phys. (Paris)* **C6-44**:503 (1983).
14. A. Rosencwaig and A. Gersho, *J. Appl. Phys.* **47**:64 (1976).
15. C. C. Huang, G. Nounesis, R. Geer, J. W. Goodby, and D. Guillon, *Phys. Rev. A* **39**:3741 (1989).
16. M. Marinelli, U. Zammit, F. Scudieri, and S. Martellucci, *Nuovo Cimento* **9D**:855 (1987).